Article:
Goycoolea, FM, Brunel, F, El Gueddari, NE et al. (7 more authors) (2016) Physical Properties and Stability of Soft Gelled Chitosan-Based Nanoparticles. Macromolecular Bioscience, 16 (12). pp. 1873-1882. ISSN 1616-5187

https://doi.org/10.1002/mabi.201600298

Full Paper

Physical properties and stability of soft gelled chitosan-based nanoparticles

Francisco M Goycoolea*, Fabrice Brunel, Nour E El Gueddari, Anna Coggiola, Giovanna Lollo, Bruno M Moerschbacher, Carmen Remuñán-López, Thierry Delair, Alain Domard and María J Alonso*

Corresponding Author(s)*

_____

Prof. F.M.G. Author-One, Dr. F.B. Author-Two, Dr. N.E.E.G. Author-Three, Prof. B.M.M.-Author-Six
University of Münster – IBBP,
Schlossplatz 8, Münster, D-48143, Germany
E-mail: fm.goycoolea@gmail.com

A.C. Author-Four, Dr. G.L. Author-Five, Prof. C.R.-L. Author-Seven,
Prof. M.J.A.-Author Ten
Universidad de Santiago de Compostela. Departamento de Farmacia y Tecnología Farmacéutica. Campus Sur s/n. Santiago de Compostela, A Coruña, 15782, Spain
E-mail: mariaj.alonso@usc.es

Dr. F.B. Author-Two, Prof. T.D. Author-Eight, Prof. A. D. Author-Nine
Laboratoire des Matériaux Polymères et des Biomatériaux – UMR CNRS 5627,
Domaine scientifique de la Doua, Bâtiment ISTIL, 15, Bd A. Latarjet, 69622, Villeurbanne Cedex Lyon, France

Abstract

In this study, we aimed to investigate the role of the degree of acetylation (DA) and of Mw of chitosan (CS) on the physical characteristics and stability of soft nanoparticles obtained through either ionic cross-linking with sodium tripolyphosphate (TPP), or reverse emulsion and subsequent gelation. Each of these methods afforded nanoparticles (NPs) or nanogels (NGs), respectively. The size of CS–TPP NPs comprising CS of high Mw (~123-266 kDa) increased with DA (~1.6 to 56%), while it did not change for CS of low Mw (~11-13 kDa); the zeta potential decreased with DA regardless of Mw (ζ ~+34.6±2.6 to ~+25.2±0.6 mV) and the NPs appeared as spheres in TEM. Stability in various cell culture media (pH 7.4 at 37ºC) was greater for NPs made with CS of DA ≥ 27%. In turn, NGs exhibited larger sizes (520±32 to 682±27 nm) than did CS–TPP NPs, and could only be formed with CS of DA < 30%. The average diameter size for these NGs showed a monotonic increase with CS's Mw. The physical properties and stability of these systems in biological media depends mostly on on the DA of CS and its influence on the balance between hydrophilic/hydrophobic

FIGURE FOR ToC_ABSTRACT

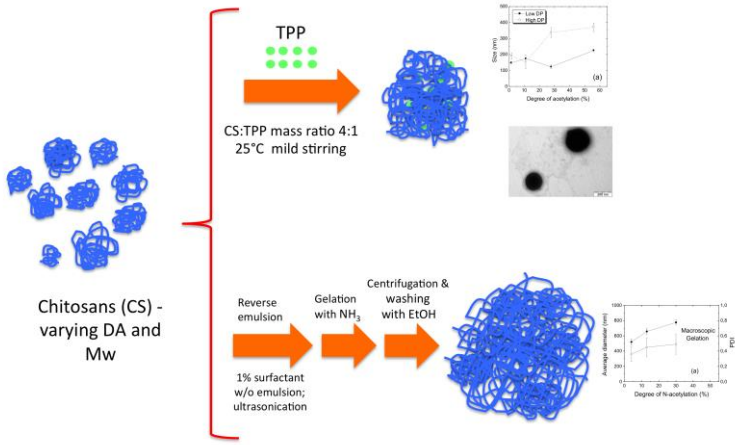

1. Introduction ((bold, 14 point font, separate all headings with an empty line))

Nanoparticles comprised of naturally-sourced polymers that can be obtained in aqueous environments have been the basis for the development of innovative materials, particularly in the pharmaceutical field as they are inherently more biocompatible than the inorganic counterparts. Chemically, chitosan (CS) is described as a family of linear aminopolysaccharide consisting of 2-deoxy-D-glucosamine (GlcN) and 2-deoxy-N-acetyl-D-glucosamine (GlcNAc) units. CS is produced by deacetylation of chitin, currently sourced from the exoskeleton of crustaceans and to a lesser extent from the cell walls of fungi. CS has received increasing attention in the last two decades, particularly in the life sciences field, due to its unique properties. From the physicochemical viewpoint, CS it has a polycationic character when dissolved in dilute aqueous acid solutions and it is amenable to physical and chemical modifications to convert it into hydrogels, scaffolds, films, fibers, and micro– and nanoparticles. In turn, it displays a range of biological activities, namely: low toxicity;[1] biodegradability by enzymes which occur ubiquitously in living organisms such as chitinase, lysozyme or human chitotriosidase;[2] mucoadhesiveness;[3] wound healing capacity;[4] and the ability to complex and subsequently deliver genetic material *in vitro* and *in vivo*.[5] *In vitro* studies also reveal that CS opens reversibly tight junctions in epithelial cell models.[6] In turn, it inhibits the growth of different types of bacteria and fungi.[7-9] In plants, CS acts as a pathogen-associated molecular pattern or a general elicitor, inducing non-host resistance and priming systemic immunity. CS presents the advantage of being recognized by plant pattern recognition receptors and triggers a panel of defense responses in several plants (mostly dicotyledonous species). These include transient production of large amounts of reactive oxygen species (oxidative burst), the increase in H^+ and Ca^{2+} influx into the cytosol, synthesis of callose (*i.e.*, reinforcement of the plant cell wall), production of antimicrobial compounds such as phytoalexins and induction of pathogenesis-related (PR) proteins.[10-12]

As the result of a uniquely wide range of properties, CS–based nanomaterials have attracted increasing attention over the recent decade. Nanoparticles have become a truly promising platform for drug delivery, particularly for transmucosal delivery via nasal, ocular, pulmonary, oral and vaginal routes.[13-14] The potential of these nanomaterials in biotechnology and other fields has only recently started to be realized. Indeed, CS–based nanomaterials are processed and handled under predominantly aqueous and fairly mild conditions. This makes them especially suitable for preserving the bioactive conformation of delicate therapeutic macromolecules (*e.g.,* peptides, hormones, antigens, pDNA, siRNA, growth factors, heparin, etc.), which otherwise would be prone to enzymatic degradation and hydrolysis. In general, polymer–based nanoparticles form by self-assembling under a bottom–up approach. Often, crosslinking of the macromolecules occurs either by physical or covalent interactions that drive the assembling process. CS–based matrix–type nanospheres (NPs) have been prepared by several different methodologies such as physical crosslinking by ionic gelation with multivalent counterions like pentasodium tripolyphosphate (TPP)[14-24] or EDTA;[25] by complex coacervation;[26,27] by emulsion/solvent evaporation;[28] by self–assembly of hydrophobically modified derivatives[29,30] or by nanoprecipitation.[31] A newly developed method has recently been documented that allows fabricating CS–based nanometric size particles without the use of a physical or covalent cross-linker, by a purely physical gelation process in a reverse emulsion, thus yielding nanogels (NGs).[32,33]

Previous studies account for the fact that the physical properties, namely the particle size distribution, polydispersity and zeta potential of CS–TPP NPs depend on the concentration of chitosan,[14] the degree of acetylation,[15-17] molecular weight[18,19] the mass ratio of chitosan:TPP,[14,19,20,22] temperature, acetic acid, the mass ratio of CS:TPP and stirring speed,[20] pH and methods of mixing,[22] salt concentration,[21,23] and time.[24] Although the experimental evidence suggests that there is a general relationship between the structural characteristics of

CS and the preparation parameters, with the physical and biological properties of chitosan-based nanoparticles, the role of the individual factors at play, still needs to be elucidated. To some extent, this is because each study is performed with chitosans from different characteristics (e.g., DA, Mw, origin, purity), and they each use different preparation protocols. In related studies, we have addressed the role of the physicochemical variables involved in the formation of CS–TPP nanoparticles for CS of varying DA and Mw.[34] The present study aims to shed light on the role of the structural characteristics of CS of CS–based nanoparticles (DA and Mw) on the physical properties and the colloidal stability in different biologically relevant environments. We compared such characteristics between nanoparticles obtained through two different preparation protocols, ionotropic gelation with sodium tripolyphosphate (TPP), and reversed emulsion gelation. By contrast with previous studies, we have used a large portfolio of fully characterized chitosans of varying DA and Mw.

2. Experimental Section

2.1. Materials

The parent CS was a sample from a batch previously obtained from squid pen chitin and supplied by Dr. Dominique Gillet of Mahtani Chitosan Pvt Ltd (France). The characteristics of this CS sample were: M_w ~435 kDa, DA 1.6% (Ref No. 113 batch No 17/12/04). All reagents were of analytical grade and unless otherwise stated, from Sigma-Aldrich Chemie (Steinheim, Germany). Deionized Milli-Q water was used throughout.

2.2. Purification, depolymerization, and N-acetylation of chitosan

The parent CS was dissolved in 5% stoichiometric excess of acetic acid and filtered successively through 3, 0.8, and 0.45 □m pore size membranes (Millipore). Purified CS was subsequently depolymerized under nitrous acid generated from $NaNO_2$ as described elsewhere[35] to obtain a series of chitosans of varying average degree of polymerization, here

designated as LDP (DP ~63-90), IDP (DP ~240-348), HDP (DP ~737-1442) and VHDP (DP ~2489). Portions of the depolymerized CS samples were N–acetylated under homogeneous conditions by adding the needed stoichiometric amount of acetic anhydride in 1,2–propanediol so as to afford chitosans of varying degrees of polymerization and DA values in the range 1.4 to 56%.

2.3. Characterization of chitosan

The molecular weight distribution of the CS samples was determined by SEC-HPLC coupled with MALLS and DRI multi-detection. The specific refractive index dn/dc values used were those estimated independently by interferometry (NFT ScanRef), and they are known to vary with the of DA of CS. The degree of acetylation of the CS samples was determined by 1H NMR spectroscopy.[36] To this end, CS was dissolved in dilute acidic D_2O (at pD 3–4) as proposed elsewhere. Spectra were recorded on a Brüker-Spectrospin AM 300 spectrometer (300 MHz). Approximately 200–250 scans per measurement were acquired.

2.4. Preparation of nanoparticles by ionotropic gelation

Nanoparticles were prepared by ionotropic gelation, in accordance with the protocol established by Calvo et al.[14] Briefly, the nanoparticles were formed spontaneously by the rapid mixing of 1.0 mL of a TPP solution into three mL of CS dissolved in 5% stoichiometric excess of acetic acid in a test tube under magnetic stirring (~200 rpm for 10 min) at room temperature. The CS:TPP mass ratio was fixed at 4:1 for all systems. The nanoparticles were isolated by centrifugation (10000 × g, 40 min, 25º C) in Eppendorf vials containing ~20 μL of glycerol, which was previously placed at the bottom of the vial.

2.5. Preparation of nanogel particles by physical gelation in reverse emulsion

Nanogels were prepared in a reverse emulsion process with a CS aqueous phase emulsified in oil, Miglyol 812N, containing the surfactant. For a typical process with 1% (w/v) of surfactant, CS (0.05g) was dissolved under moderate stirring by adding acetic acid in a

stoichiometric amount with respect to the free amine functions for each degree of N-acetylation. This aqueous CS solution (5 mL, 1 %, w/v) was emulsified in 25 mL (23.75 g) of Miglyol 812N containing Span 80 (0.25 g, 1 %, w/v) with a sonotrode (Bandelin KE76) operating at 20 kHz with a peak-to-peak magnitude of 260 µm under magnetic stirring. The ultrasonic probe (Ø = 6 × L = 118 mm) was immersed into the liquid up to 2 cm. The reactor was thermostated to prevent flocculation and destabilization of the emulsion due to the heating induced by sonication. After 5 min of ultrasound treatment, a stream of ammonia increased the pH of the medium, which caused the gelation of CS droplets. The ultra-sound treatment was maintained for 10 min to prevent droplet coalescence and/or particle aggregation. Finally, the dispersion was centrifuged at 1000 x g for 15 min. After the elimination of the supernatant, the particles were dispersed in 40 mL of ethanol. This washing cycle was repeated twice with ethanol and twice with water, and then the particles were dispersed in an ammonium acetate buffer (50 mmol/L pH = 4.5) by slow stirring overnight, the final pH was measured between 5.5 and 6.5.

2.6. Physical characterization

The size distribution of the nanoparticles was determined by dynamic light scattering using non-invasive back scattering (DLS-NIBS, measuring angle 173º) using a Malvern Zetasizer NanoZS ZEN 3600 (Malvern Instruments UK) equipped with a 4mW He/Ne laser beam operating at λ=633 nm. All measurements were performed at 25º ± 0.2 ºC. The zeta potential (ζ) was measured by mixed laser Doppler velocimetry and phase analysis light scattering (M3–PALS) using the same instrument as for size determination. The value of ζ was derived using Smolouchowski's equation from the electrophoretic mobility measurements. The ultrastructure of the nanoparticles was investigated by transmission electron microscopy TEM on a Philips CM12 instrument (Eindhoven, The Netherlands). Transmission electron

micrographs (TEM) of CS–TPP nanoparticles were obtained after the deposition of the nanoparticle suspensions in copper grids coated with a Formvar® membrane and using negative contrast staining with phosphotungstic acid 2 % (w/w).

2.7. Stability in various buffer and cell culture media

The colloidal stability of the nanoparticles and nanogels was investigated from the evolution of the particle size distribution over time during incubation in the following media and conditions: a) Roosevelt Park Memorial Institute (RPMI-1640) medium (PAA Laboratories GmbH, pH 7.34) supplemented with 6% (v/v) fetal bovine serum (PAA Laboratories GmbH), 1% (v/v) L-glutamine and 0.2%(v/v) penicillin/streptomycin solution (GPS, Sigma-Aldrich) at 37°C; b) OptiMEM® (pH 7.30) medium (GIBCO Invitrogen Corp.) at 37°C; c) Oxidative burst medium (OBM) (pH 5.90) at 37°C; d) Antifungal activity medium (AAM) (pH 5.50) at 28°C; e) Nutrient yeast glucose medium (NYG) pH 5.90 at 37°C; f) Water-glycerol at 4°C; g) Phosphate buffer 50 mM (pH = 7.40; 4ºC); h) NaCl 150 mM at 4°C; i) ammonium acetate buffer (pH 4.50) at 37°C; j) Complete medium (pH 4.30) at 37°C. To this end, an aliquot of the various nanoparticle systems was added to a measuring cuvette containing the buffer/media equilibrated to the desired temperature, and the size measurements were registered at varying time intervals during incubation (media a-e). In the case of stability during long-term storage under refrigeration at ~4 ˚C (media f-i), size measurements by DLS-NIBS were registered on aliquots of the stored nanoparticle solutions and mesured at 25 ˚C.

3. Results and Discussion

Sixteen samples of purified biomedical–grade CS were prepared from the same parent batch of chitosan, previously obtained from chitin isolated from squid pen. They differed in their degree of polymerization and DA. As shown in Table 1 this set of samples spans a broad

range of Mw (~10 to ~400 kDa) and degrees of acetylation (DA 1.4 to 56%). Along with the degree of polymerization, the DA is a fundamental parameter that directly determines the physicochemical and biological properties of chitosan. Therefore, we hypothesized that the ability to process chitosan into gelled colloidal nanoparticles and their physical and stability properties would be influenced by such parameters.

3.1. Physical properties of CS – TPP nanoparticles

The first class of nanoparticles addressed in this study were obtained by ionotropic gelation of CS (using samples of type LDP and HDP, Table 1) with TPP and according with the original protocol developed by the USC (Spain) group. Chemically, the interaction of CS with TPP is regarded to be mediated by the intramolecular ionic crosslinking caused by tripolyphosphoric counterion species (*e.g.,* $P_3O_{10}^{5-}$, $NaP_3O_{10}^{4-}$ and $Na_2P_3O_{10}^{3-}$), product of the dissociation of TPP in aqueous solution at a given pH, with protonated $-NH_3^+$ groups in CS. The effect of pH, ionic strength, processing conditions and type of CS on the physical characteristics of CS–TPP nanoparticles, has been addressed in independent studies.[14-25,34] In the present study, it was possible to obtain particles with processing yields varying in the range ~27–47% for both samples of LDP CS and HDP CS, respectively, as shown in **Figure 1**. Interestingly, the production yield of particles for the different type of CS exhibited a gradually decreasing trend with increasing DA values and attained lowest values for DA~27%. At the highest DA (~51-56%), the production yield increased noticeably. The clear negative dependence of the processing yield with increase in DA within the range of DA ~ 0–27%, irrespective of the M_w of CS, suggests that nanoparticles formation depends not only on the electrostatic interactions between $-NH_3^+$ groups and phosphate ionic species, which determine the extent of crosslinking, but also on other contributions such as H-bonding, hydrophobic association and on other structural features of CS. In agreement with this suggestion, if we consider that at a fixed mass ratio of CS to TPP, there is an increase in N-acetylated residues (which occurs at

the expense of D-glucosamine ones during N-acetylation), it means that the net charge ratio of $–NH_3^+$ to phosphate groups decreases. In a related study,[34a] we have shown that the dependence of the physical characteristics and yield of formation of nanoparticles on the molar ratio of $–NH_3^+$ to TPP is highly influenced by CS's DA and does not describe a unique trend of behavior. The results of the present study are consistent with those of the our previous study in that as the DA increases (up to 47%) the yield of nanoparticles production decreases. In an ongoing study, we are addressing the role of the degree of acetylation, molecular weight and concentration of chitosan, and the ionic strength of the solvent, on the particle size of chitosan-tripolyphosphate nanoparticles.[34b] The increase in production yield observed for the CSs of very high DA in the present study is consistent with the proposal that the net electrostatic cross-linking of $–NH_3^+$ is not the only mechanism that governs the behavior of these systems, but cooperative effects must also contribute to their overall cross-linking. The disruption of the formation of cooperative junction zones involving locally ordered polymer stretches of neighbouring glucosamine residues crosslinked by TPP ions, may account for the gradual reduction in the yield of nanoparticles formed. This effect seems to be favored as the proportion of N-acetyl-glucosamine residues augments up to DA ~ 27%. At higher DA values though, the contribution of hydrophobic effects brought in by the large proportion of N-acetyl-glucosamine residues, is consistent with an increase in the overall production yield, the consequence of a complementary association mechanism concomitant to the ionic cross-linking. This hypothesis is in overall agreement with the results from hydrodynamic size measurements as will be discussed below. The process of the formation of the CS–TPP nanoparticles can be envisaged as the consequence of a sol–to–gel process governed by essentially the same general mechanisms as those underlying the setting up of a macroscopic, percolated, three–dimensional polymer gel network. However, by contrast with macroscopic gel systems, nanoparticle gelation occurs in conditions that avoid gel percolation throughout the continuous phase. It was also interesting to note that in nanoparticles

comprising low–Mw CS of low DA (DA < 11%) resulted in a significant ($p \leq 0.05$) higher yield of production than those of high–Mw CS. Meanwhile, this tendency is reversed for the particles comprising CS of high DAs. The increase in yield for systems of low–M wand low DA is consistent with the notion that the shorter CS species tend to form more densely-packed particles than those comprised by high Mw. This is mostly favored for the short, low DA CS species, bound to adopt a more rigid rod–like conformation, than the high DA CS of greater chain flexibility.[37]

Figure 2 depicts the variation of particle size with CS's DA for CS-TPP ionically cross-linked nanoparticles. A close inspection of **Figure 2a** reveals that the average diameter of the particle did not change with the CS's DA in the interval DA ~1.4 to 51 % for nanoparticles prepared from LDP CS, and only the nanoparticles made of CS of DA 27% were significantly ($p \leq 0.05$), albeit only slightly, smaller than the rest. A very different trend in this respect was observed for nanoparticles harnessed from HDP CS that show a monotonic increasing size from ~150-190 nm to two-fold larger (~300-350 nm) from the low to the high end of DA, respectively.

In turn, **Figure 2b** shows the variation of ζ values with DA for both LDP CS and HDP CS. A closer inspection of the plot reveals a rather uniform decrease of ζ values for LDP CS from ~+35 to ~+27 mV. Nanoparticles obtained from HDP CS exhibited a slight increment (~+32 to ~+37 mV) in ζ as DA increased from 1.6 to 27.5 %, and a drastic drop as the DA rose to 56%. These results are consistent with the idea that the presence of N–acetyl groups in CS leads to the creation of more expanded structures, perhaps due to the formation of 'loops' formed at the NP's surface by local CS chain segments where TPP does not form cooperative crosslinking bridges between $–NH_3^+$ groups in D–glucosamine residues. The formation of these types of structure has been proposed to explain the effect of pH on the degree of protonation of $–NH_3^+$ groups in CS–TPP gel beads[38] and also to account for differences in

size and zeta potential found in CS-based nanocapsules comprising CS of LDP and HDP and varying DA.[39]

The tendency to form 'loops' at the NP's surface would be expected to be more favored in larger CS chains than in shorter ones that can be conceived as more densely packed (Figure 2a). In turn, the consequence of the formation of these 'loops' in HDP CS nanoparticles may lead to the creation of zones of greater local hydrophobicity, that would preferably be oriented towards the inner side of the nanoparticle matrix. This hypothesis agrees well with the marginal increment observed in ζ with DA up to DA 27% (Figure 2b). The decrease in ζ of nanoparticles of HDP CS of DA 56% may reflect that a different structural rearrangement takes place in these nanoparticles as they are unable to accommodate all the hydrophobic, neutral groups inwards. Interestingly, when the nanoparticles are produced in NaCl 85 mM, and the stoichiometry of amino functions to TPP (NH_3^+/TPP molar ratio) is fixed,[34a] the influence of the DA on the size of CS-TPP NPs is very different. In this case, the particle size of nanoparticles comprising high DA CS is smaller than those comprising the polymer of lower DA. An explanation for this may stem from the varying stoichiometry of crosslinking that is assessed on CS-TPP NPs when the mass CS/TPP ratio is kept fixed, and the DA of the constituent CS increases (*i.e.* the NH_3^+/TPP molar ratio effectively decreases).

With regards to the dependence of the zeta potential (ζ) on CS's DA, a comparison with data from a related study,[34a] shows that in 85 mM NaCl and fixed molar ratio NH_3^+/TPP molar ratio (=12 or 14), the values of ζ decrease linearly in the range of DA 0 to 30% down to a minimum value of DA beyond which no further change is observed upon increasing DA. This is consistent with the notion that in water, a reduction in chain stiffness favors the formation of the hypothesized 'loops' in the HDP CS that also influence the size dependence discussed above and entail the characteristic observed profile.

In turn, in LDP CS–based nanoparticles, the decreasing tendency in zeta potential may be only a consequence of the lower proportion of net charged $–NH_3^+$ groups in the system that

are evenly distributed on the surface and inner matrix of the nanoparticle. The morphology of the nanoparticles was invariably spherical as evidenced by representative TEM micrographs (**Figure 3**). It can be appreciated that nanoparticles obtained from LDP CS (**Figure 3a**) appear as more dense and compact than those obtained from HDP CS at equivalent DA (**Figure 3b**). In turn, nanoparticles of HDP CS of high DA (**Figure 3c**) appear as larger structures in general accordance with results and interpretations from DLS-NIBS measurements shown in Figure 2a.

3.2. Stability of CS–TPP nanoparticles

The evolution of the particle size distribution of CS-TPP NPs during incubation in different media commonly used for bioactivity assays was studied using DLS-NIBS and by visual inspection to monitor the formation of aggregates. NPs prepared from eight different types of CS samples of either LDP or HDP and varying DA were all tested upon incubation in several media relevant to bioactivity assays. Namely, in RPMI-1640 cell culture medium (pH 7.40 at 37ºC) supplemented with 6% (v/v) fetal calf serum and other essential nutrients and necessary components; plant oxidative burst medium (OBM; pH 5.90; 37ºC); antifungal activity medium (AAM; pH 5.99 at 37ºC) and in water/glycerol during long-term storage at 4ºC. RPMI-1640 is a medium used for the cultivation of human cell lines that grow either adhered to a plastic surface as monolayers or in suspension, such as normal and neoplastic leukocytes, including fresh lymphocytes and dendritic cells. OBM is a medium typically used in plant bioactivity studies. For one of the NP systems (LDP-9) the stability was also tested in OptiMEM® (pH 7.30 at 37ºC) and in NYG (pH 5.90 at 37ºC) antibacterial activity media. OptiMEM® reduced-serum medium is a modification of Eagle's minimum essential medium (EMEM), buffered with HEPES and sodium bicarbonate and supplemented with hypoxanthine, thymidine, sodium pyruvate, L-glutamine, trace elements and growth factors. It

is used in gene transfection *in vitro* studies. NYG is a medium commonly used in antibacterial assays. **Table 2** summarizes the results of the stability studies.

It can readily be noticed that in RPMI-1640 medium, NPs made with LDP chitosan were clearly more stable as the DA increased from DA 1.0 to 51%. Meanwhile, NPs comprising chitosan, with a high degree of polymerization (HDP) and low DA (1.6 or 11%), aggregated immediately and only those comprising CS of DA ≥ 27% were stable. These results are in good agreement with those obtained in previous related studies, where nanocapsules were coated with the same chitosan samples as those used here, for CS-TPP nanoparticles.[30,38] In such studies, it was found that LDP nanocapsules showed greater stability in supplemented RPMI-1640 and in NaCl, at concentrations close to physiological conditions (~150 mM) at DA varying between ~1 and 51% than did nanocapsules comprising HDP chitosan. Nanocapsules comprising HDP chitosan of DA 27 and 56% were considerably more stable than those of lower DA. As in the case of nanocapsules, the observations of the present study on matrix-type NPs are consistent with the notion that the greater DA of CS induces a more hydrophilic surface in CS-TPP nanoparticles, hence, the critical concentration of electrolytes needed to achieve a colloidal suspension, mediated by repulsive hydration forces attained at the surface and the hydrated ions surrounding it, is lower than that for a more hydrophobic topology.[40] Moreover, adsorbed proteins are also known to modify the hydration shell and stability of colloidal nanoparticles.[39-42]

Stability in a plant's oxidative burst medium revealed that the more stable nanoparticles were also those fabricated with CS of DA ≥ 27%. However, in this case, for nanoparticles comprising LDP-1 chitosan the onset of aggregation was after ~20 min of incubation, in contrast to the ones with HDP-1 chitosan that aggregated immediately. In turn, in AAM, only the nanoparticles containing chitosans of DA ≥ 27.0% were stable regardless of the DP of CS. In the NYG antibacterial medium, only the nanoparticles made with LDP-9 were tested and showed fairly limited stability (~25 min). Future studies are needed to assess whether

nanoparticles made with chitosans of higher DA are stable in this and other antibacterial media (*e.g.,* LB medium). The results in OBM and AAM are in reasonably good keeping with those observed in RPMI-1640 and again reflect that the stability in biological fluid media in general, is promoted for chitosans of a high degree of acetylation, that in turn leads to the creation of a more hydrophilic surfaces, as discussed above.

All the CS–TPP nanoparticles comprising the series of LDP and HDP chitosans of varying DA were stable during refrigeration storage in water/glycerol (~70/30 v/v) at 4ºC. Glycerol exerts a protective effect against aggregation. This is a finding that has potential practical value in future studies addressing the biological properties of these nanoparticles.

3.3. Physical properties of nanogels obtained by gelation reverse emulsion

The second class of nanoparticles addressed in this study were produced in the absence of any crosslinking agent and by exploiting the capacity of CS to set up consolidated gel networks under tightly controlled physicochemical conditions. The formation of physical hydrogels requires i) the alteration of the CS solubility, in such a way that solvent-segment interactions be reduced to favor segment-segment interactions, and ii) a polymer concentration to be initially above the critical gelling concentration, C_o, so that a network can be formed. Reducing CS solubility will be achieved by decreasing the repulsive electrostatic interactions between the macromolecules, and this can be obtained by lowering the charge density of CS or by modifying the dielectric constant of the medium. In this regard, Montembault *et al.*[43] reported an approach to harness macroscopic physical gels of CS without using potentially toxic chemicals. The charge density of the CS chains was decreased by deprotonation of the NH_3^+ groups with gaseous ammonia. To create physical nanohydrogels, using this gelation process, the CS solution was emulsified into a continuous oil phase containing a surfactant, before triggering the ammonia-induced gelation. Hence, the gelation of CS, segregated into aqueous droplets, leads to the formation of gelled nanoparticles.

In a preceding study,[32] we reported the structural properties of chitosan nanogels. These were extended here to address the role of the DA of chitosan and the Mw. The influence of the degree of N-acetylation (DA) of CS on the particles size is shown in **Figure 4a**. The observed particle sizes increase when the DA rose up to 30 %, and only macroscopic gelation was obtained beyond this DA. This result could be due to the increment of the macromolecular chain hydrophobicity with the DA. The first consequence is that the hydrocarbon chains of the surfactant could adsorb at the interface of the droplets rather than expand toward the continuous phase. The reduction of the steric stabilization would thus explain the colloidal instability and aggregation. A second explanation could be a lower segregation of the hydrophobic CS in the droplets. The macromolecular chain could be present, or at least partially solubilized, in the organic phase leading to a macroscopic gelation or an entanglement of the polymer chain from different droplets.

Figure 4b reports the impact of the degree of polymerization of CS on the particle size distribution. The best-defined CS nanoparticles, regarding particle size and polydispersity, could be obtained with a lower DP. Furthermore, the standard deviation sharply increased above a critical degree of polymerization (DP~400), suggesting that in this case, the formed nanoparticles had too high a broad particle size distribution which did not allow accurate sizing. This particular behavior could be related to the high viscosity of the dispersed phase which increases exponentially with the Mw of CS. By increasing the viscosity of the dispersed phase the droplet disruption energy also increases leading to ill-defined materials.

In previous studies,[33] we showed that nanogels obtained from high Mw chitosan (Mw=400 000 $g.mol^{-1}$) had a spherical morphology as revealed by TEM, comparable to that of the CS–TPP nanoparticles (Figure 3), and a size range that lay within the range of size measurements by DLS-NIBS.

3.4. Stability of nanogels obtained by gelation reverse emulsion

CS nanogels obtained by reverse emulsion and alkali gelation exhibited a very long-term colloidal stability in ammonium acetate buffer (50 mM pH = 4.5) and in NaCl 150 mM during storage at 4 ºC as shown in Table 3. This stabilization was attributed to both electrostatic and steric mechanisms due to the expanded protonated chains of chitosan at the colloid interface, as discussed in previous studies.[30] By contrast, in a phosphate buffer at pH 7.40, the nanohydrogels aggregated immediately, which was in line with the results observed for CS–TPP NPs. In oxidative burst medium (pH = 5.90), the nanohydrogels were stable only for a short period (< ~20 min), while in the complete medium (pH = 4.30), they remained stable for less than one week. The observed results indicate that the neutralization of the charges of chitosan at the surface of the nano gels, as the pH increases, is the main driving force that leads to the collapse of the interfacial chitosan, and hence to the aggregation of the colloid. In the presence of 150 mM NaCl, the stabilization of the system could be attributed to repulsive hydration forces attained at the surface. This explanation is in line with the above-explained mechanisms, which are proposed to operate in CS–TPP NPs and nanocapsules.[39] It is interesting to notice that the presence of divalent ions in the complete medium did not induce aggregation as compared to a phosphate buffer, where aggregation was presumably driven by phosphate ions. Also, the higher viscosity of the complete medium could also have contributed to a slowdown in the aggregation rate. The colloidal stability of nanogels in different biological media was studied and compared to that used for CS–TPP nanoparticles, except for OBM, which was common to both types of systems. In both nanostructures for comparable chitosan samples used to harness them (LDP DA 4 and LDP DA 1 in CS–TPP NPs and nanoneedles, respectively), similar stability was observed. Based on these results, we argue that the colloidal stability of both types of nanosystems is governed by similar phenomena.

4. Conclusion

The present study has allowed us to glean a further understanding of the often neglected impact of chitosan structural characteristics (DA and Mw) on the physical properties (size and zeta potential) and stability in biologically relevant media of soft, ionically and physically crosslinked gelled nanoparticles based on chitosan. It has become clear that the physical dimensions, stability, and, to some extent, the surface electrical charge of these systems can be tuned by appropriate choice of chitosan's properties and protocol of fabrication. Hence, our work will serve as a guide of future studies aimed to further address the application of these systemsin biomedicine, agriculture, and other fields. In recent studies, we have evaluated the interaction between CS–TPP NPs and mammalian cells and their possible fate as well as their degradation, using a FRET approach.[44] Future such type of studies are needed for CS-based nanomaterials furnished from CS of varying structural characteristics.

Acknowledgments: Financial support of the European Union from the NANOBIOSACCHARIDES project (Ref No. 013882 of call FP6–2003–NMP–TI–3–Main) is gratefully acknowledged.

Received: Month XX, XXXX; Revised: Month XX, XXXX; Published online:
((For PPP, use “Accepted: Month XX, XXXX” instead of “Published online”)); DOI: 10.1002/marc.((insert number)) ((or ppap., mabi., macp., mame., mren., mats.))

Keywords: chitosan, nanoparticles, nanogels, reverse emulsion, ionotropic gelation

[1] T. T. Chandy, C.P. Sharma, *Biomater. Artif. Cells Artif. Organs,* **1990,** *18*, 1

[2] T. Kean, M. Thanou, *Adv. Drug Deliv. Rev.,* **2010,** *62* 3

[3] I. A. Sogias, A. C. Williams, V. V. Khutoryanskiy, *Biomacromoleclues,* **2008,** *9,* 1837

[4] C. Chatelet, O. Damour, A. Domard, *Biomaterials,* **2001,** *22,* 261

[5] K. Roy, H. Q. Mao, S. K. Huang, K. W. Leong, *Nat. Med.,* **1999,** *5,* 387

[6] J. Smith, E. Wood, M. Dornish, *Pharm. Res.,* **2004,** *21,* 43

[7] X. F. Liu, Y. L. Guan, D. Z. Yang, Z. Li, K. D. Yao, *J. Appl. Polym. Sci.,* **2001,** *79,* 1324

[8] E. I. Rabea, M. E. Badawy, C. V. Stevens, G. Smagghe, W. Steurbaut, *Biomacromolecules*, **2003,** *4,* 1457

[9] S. Sekiguchi, Y. Miura, H. Kaneko, S. I. Nishimura, N. Nishi, M. Iwase, S. Tokura, in *Food Hydrocolloids: Structures, Properties and Functions: Proc. Int. Conf. and Industrial Exhibition on Food Hydrocolloids,* (Eds: K. Nishinari, E. Doi), Plenum Press, New York, **1993,** p. 71

[10] P. Vander, K. M. Vårum, A. Domard, N. E. El Gueddari, B. M., Moerschbacher *Plant. Physiol.,* **1998,** *118,* 1353

[11] I. Ortmann, G. Sumowski, H. Bauknecht, B. M. Moerschbacher, *Physiol. Plant Pathol*., **2004,** 227

[12] H. Kauss, W. Jeblick, A. Domard, A. J. Siegrist, in *Advances in Chitin Science,* Vol. III*,* (Eds: A. Domard, G. A. F. Roberts, K. M. Vårum), Jaques Andre Publisher, Lyon, **1997,** p. 94

[13] M. García–Fuentes, M. J. Alonso, *J Control. Release,* **2012,** *161*, 496

[14] P. Calvo, C. Remuñán-López, J. L. Vila-Jato, M. J. Alonso, *J. Appl. Polym. Sci., **1997,** 63,* 125

[15] H. Zhang, M. Oh, C. Allen, E. Kumacheva, *Biomacromolecules,* 2004, *5,* 2461

[16] M. Huang, E. Khor, L.-Y. Lim, *Pharm. Res., 2004, 21,* 344

[17] Y. Xu, Y. Du, *Int. J. Pharm.,* **2003,** *250,* 215

[18] K. A. Janes, M. J. Alonso, *J. Appl. Polym. Sci.,* **2003,** *88,* 2769

[19] Q. Gan, T. Wang, C. Cochrane, P. McCarron, *Colloid. Surface. B.,* **2005,** *44,* 65

[20] W. Fan, W. Yan, Z. Xu, H. Ni, *Colloid. Surface. B,* **2012,** *90,* 21

[21] H. Jonassen, A. L. Kjøniksen, M. Hiorth, *Colloid Polym. Sci.* **2012,** *290,* 919

[22] A. Nasti, N. M. Zaki, P. Leonardis, S. Ungphaiboon, P. Sansongsak, M. G. Rimoli, N. Tirelli, *Pharm Res.*, **2009,** *26,* 1918

[23] Y. Huang, Y. Lapitsky, *Langmuir,* **2011,** *27,* 10392

[24] A. Rampino, M. Borgogna, P. Blasi, B. Bellich, A. Cesàroa, *Int. J. Pharm.,* **2013,** *455,* 219

[25] B. Loretz, A. Bernkop–Schnürch, *AAPS J,* **2006,** 756

[26] A. Drogoz, L. David, C. Rochas, A. Domard, T. Delair, *Langmuir,* **2007,** *23,* 10950

[27] C. Schatz, A. Domard, C.Viton, C. Pichot, T. Delair, *Biomacromolecules,* **2004,** *5,* 1882

[28] Y. Hu, X. Jiang, Y. Ding, H. Ge, Y. Yuan, C. Yang, *Biomaterials,* **2002,** *23,* 3193

[29] M. Lee, Y. W. Cho, J. H. Park, H. Chung, S. Y. Jeong, K. Choi, D. H. Moon, S. Y. Kim, I.-S. Kim, I. Kwon, *Colloid Polym. Sci.,* **2006,** *284,* 506

[30] J. P Quiñones, K. V. Gothelf, J. Kjems, C. Yang, A. M. H. Caballero, C. Schmidt, C. Peniche-Covas, *Carbohydr. Polym.* **2013,** *92,* 856

[31] A. G. Luque-Alcaraz, J. Lizardi, F. M. Goycoolea, M. A. Valdez, A. L. Acosta, S. Iloki-Assanga, I. Higuera-Ciapara, W. Argüelles-Monal *J Nanomaterials*, **2012,** Article ID 265161

[32] F. Brunel, L. Veron, L. David, A. Domard, T. Delair *Langmuir,* **2008,** *24,* 11370

[33] F. Brunel, L. Veron, C. Ladaviére, L. David, A. Domard, T. Delair *Langmuir,* **2009,** *25,* 8935

[34] a) H. Kleine-Brueggeney, G. K. Zorzi, T. Fecker, N.E. El-Gueddari, B. M. Moerschbacher, F. M. Goycoolea *Colloid. Surface. B*, **2015,** *135,* 99; b) S. Sreekumar, N.E. El Gueddari, F. M. Goycoolea, B. M. Moerschbacher, G. R. Rivera-Rodriguez, unpublished

[35] G. G. Allan, M. Peyron, in *Chitin Handbook,* (Eds: R. A. A. Muzzarelli, M. G. Peter), Grottammare Atec, Italy, **1997,** p. 175

[36] A. Hirai, H. Odani, A. Nakajima *Polym. Bull.* **1991,** *26,* 87

[37] R. Novoa-Carballal, E. Fernández-Megia, R. Riguera, *Biomacromolecules,* **2010,** 11, 2079

[38] F. L. Mi, S. S. Shyu, S. T. Lee, T. B. Wong *J. Polym. Sci. Po.l Phys.,* **1999,** *37,* 1551

[39] M. J. Santander-Ortega, J. M. Peula-García, F. M. Goycoolea, J. L. Ortega-Vinuesa, *Colloid. Surface. B,* 2011, **82** 571–580

[40] M. J. Santander-Ortega, M. V. Lozano-Lopez, D. Bastos-Gonzalez, J. M. Peula-Garcia, J. L. Ortega-Vinuesa, *Colloid Polym. Sci.,* **2009,** *288,* 159–172

[41] J. M. Santander-Ortega, A. B. Jodar-Reyes, N. Csaba, D. Bastos-Gonzalez, J. L. Ortega-Vinuesa *J. Colloid Interf. Sci.* **2006,** *302,* 522

[42] J.A. Molina-Bolivar, J.L. Ortega-Vinuesa *Langmuir* **1999,** *15,* 2644–2653

[43] A. Montembault, C. Viton, A. Domard, *Biomaterials* **2005,** *26,* 1633

[44] J.P. Fuenzalida, T. Weikert, S. Hoffmann, C. Vila-Sanjurjo, B. M. Moerschbacher, F. M. Goycoolea, *Biomacromolecules*, *15*, 2532–2539

The degree of acetylation and the molecular weihght of chitosan have a direct influence on the size, zeta potential and stability of chitosan-based nanoparticles. This was evidenced in ionically crosslinked nanoparticles and in nanogels produced by reverse emulsion. The ionically crosslinlked particles are far more stable when the degree of acetylation of chitosan increases (up to 56 %).

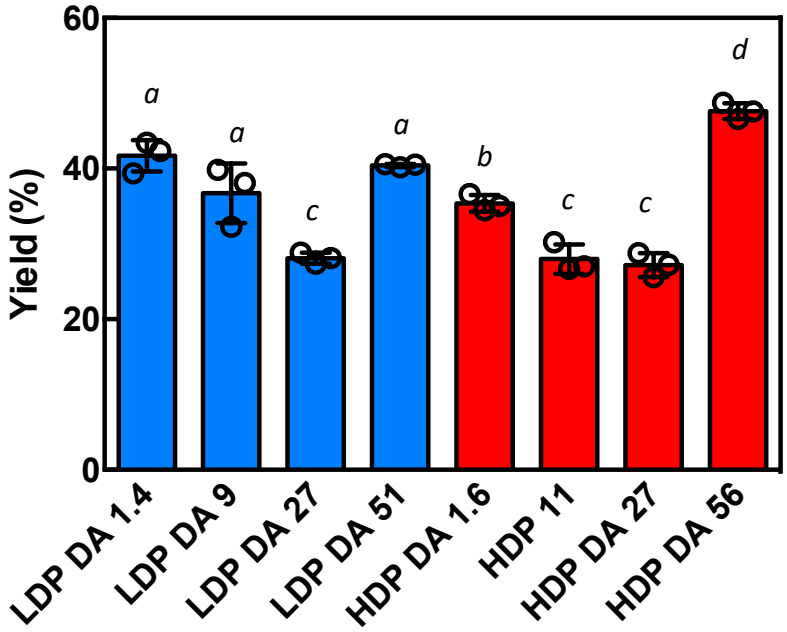

Figure 1. Production yield of chitosan–TPP nanoparticles as a function of chitosan's degree of N-acetylation of low (M_w ~10 kDa) and high (Mw~120 kDa) degree of polymerization (as indicated in legend; CS:TPP mass ratio was fixed to 4:1; water) (mean average values ± SE; different letters in symbols denote significant diferences among treatments $p \leq 0.05$; n=3).

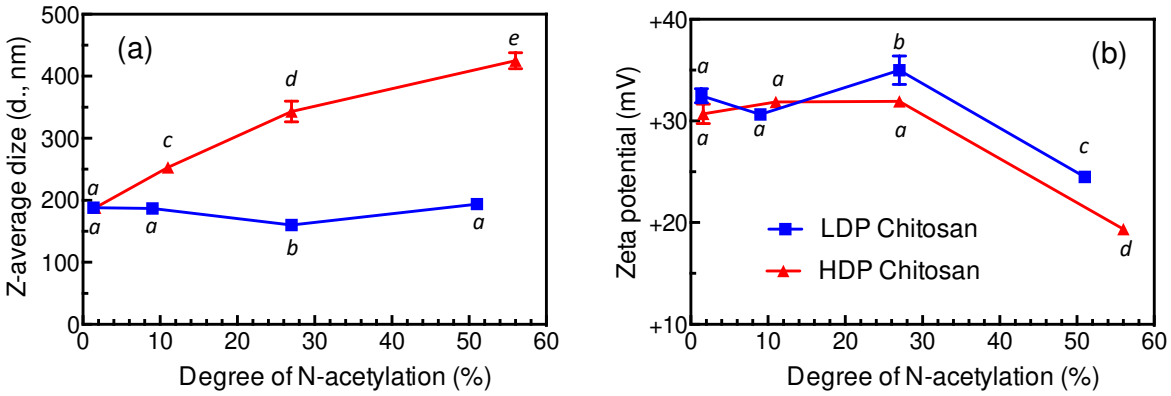

Figure 2. Variation of a) Z-average size and b) Zeta potential of chitosan-pentasodium tripolyphosphate (CS-TPP) nanoparticles, isolated and re-suspended, with the degree of acetylation of chitosan of low degree of polymerization (DP~58-82) and of high degree of polymerization (DP ~ 776 - 1442) degree of polymerization (as indicated in legend; CS:TPP mass ratio was fixed to 4:1; water; mean average values ± SE; different letters in symbols denote significant diferences $p \leq 0.05$, $n=3$).

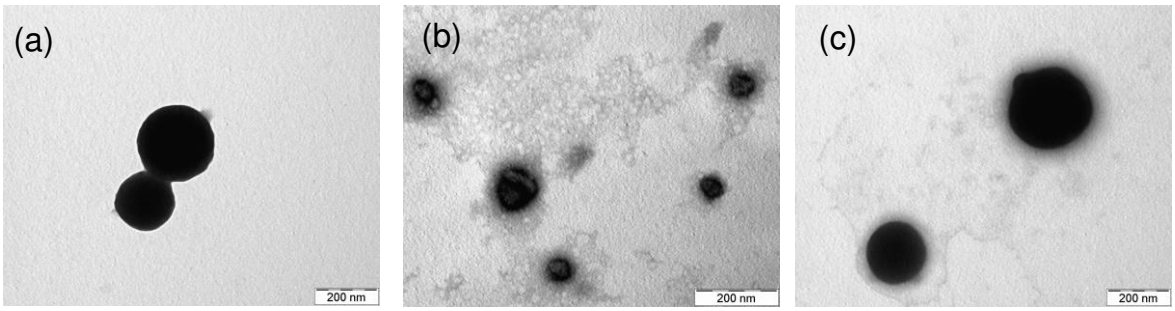

Figure 3. TEM micrographs of chitosan–TPP nanoparticles prepared from chitosan of varying M_w and DA: a) LDP DA 9.2%; b) HDP DA 11% and c) HDP DA 56%. The nanoparticles were stained with phosophotungstic acid 2 % (w/w).

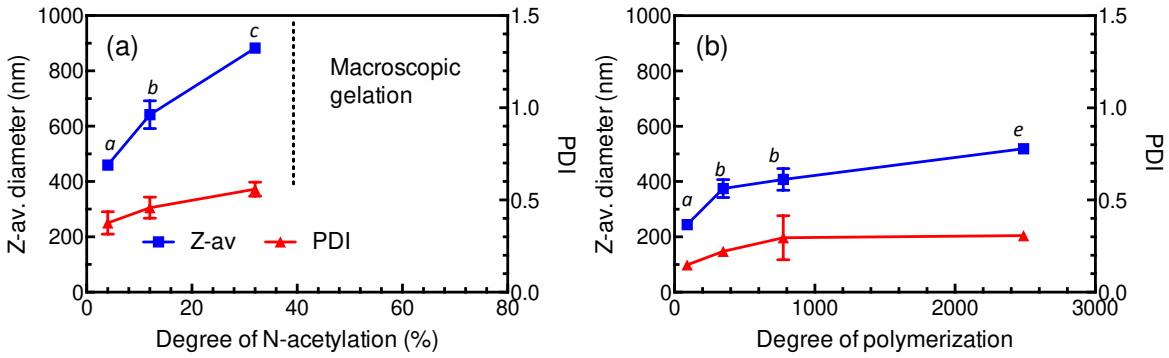

Figure 4. Average diameter (•) and polydispersity index (□) of CS-nanoparticles as a function of: (a) the degree of N-acetylation (Mw = 405400 ± 8 800; DP 2489) and (b) the degree of polymerization (DA = 4%) of chitosan (mean average values ± SE; different letters in symbols of diameter values denote significant diferences $p \leq 0.05$, $n=6$).

Table 1. Physicochemical characteristics of chitosan samples.

Sample Code	Degree of N-acetylation [mol %][a]	M_w [b]	M_n[b]	I_p[b]	DP[c]
VHDP-4	4.0	406000	305300	1.33	2489
VHDP-13	13.0	406000	305300	1.33	2489
VHDP-30	30.0	406000	305300	1.33	2489
VHDP-45	45.0	406000	305300	1.33	2489
HDP-1	1.6	123900	89000	1.39	766
HDP-4	4.0	126400	81800	1.54	776
HDP-11	11.0	122100	75330	1.62	737
HDP-27	27.5	143000	85710	1.67	818
HDP-56	56.0	266100	139700	1.90	1442
MDP-4	4.0	56700	34800	1.63	348
MDP-4b	4.0	39100	22200	1.76	240
LDP-1	1.4	13200	11130	1.19	82
LDP-4	4.0	14900	7450	2.00	90
LDP-9	9.2	9572	5914	1.62	58
LDP-27	27.1	11530	8120	1.42	67
LDP-51	51.0	11420	6012	1.90	63

[a] Degree of N-acetylation as determined by ^{1}H NMR spectroscopy; [b] Parameters determined by GPC–HPLC with multidetection (MALLS–DRI): weight average molecular weight (M_w); number average molecular weight (M_n); polydispersity index ($Ip = M_w/M_n$); [c] Degree of polymerization (DP = M_w /molar mass per residue)

Table 2. Colloidal stability of chitosan nanoparticles obtained by ionotropic gelation with sodium tripolyphosphate (CS–TPP) after incubation in various media[a,b]

Media[c]	Chitosan sample							
	LDP-1	**LDP-9**	**LDP-27**	**LDP-51**	**HDP-1**	**HDP-11**	**HDP-27**	**HDP-56**
RPMI-1640 (pH 7.40; 37ºC)	I.A.	< 1 h	< 6 h	> 21 h	I.A.	I.A.	> 21 h	> 21 h
OptiMEM (pH 7.45, 37ºC)		< 1 h						
OBM (pH = 5.90, 37ºC)	< 20 min	< 2 h	> 3 h	> 3 h	I.A.	> 3 h	> 3 h	> 3 h
AAM at (pH = 5.99; 28°C)	I.A.	I.A.	< 1 h	> 48 h	I.A.	I.A.	> 48 h	> 48 h
NYG (pH 5.90, 37ºC)		< 25 min						
Water (4°C)	> 4 months	> 4 months	> 4 months	> 4 months	> 4 months	> 4 months	> 4 months	> 4 months

[a] CS:TPP mass ratio 4:1; [b] The values in Table indicate either the maximal time (values proceeded by "<") before the onset of aggregation or the minimal time (values preceeded by ">") that particles remained stable during incubation at the given temperature; I.A denotes immediate aggregation. Blank cells denote non tested assays.; [c] HBSS: Henk's bufffer saline solution; RPMI: Rossevelt Park Memorial Institute medium; OBM: Oxidative burst medium; AAM: Antifungal activity medium; NYG: Nutrient yeast glucose broth.

Table 3. Stability of nanogels obtained by reverse emulsion during incubation in various media[a]

	Media[b]				
Chitosan	**Phosphate buffer 50 mM (pH 7.40; 4ºC)**	**NaCl 150 mM (4ºC)**	**Ammonium acetate buffer 50 mM (pH 4.50; 4°C)**	**OBM (pH = 5.90; 37ºC)**	**Complete medium (pH 4.30; 37°C)**
LDP-4	I.A.	> 3 months	> 3 months	< 20 min	< 1 week

[a] The values in Table indicate either the maximal time (values preceeded by "<") before the onset the of aggregation or the minimal time (values preceeded by ">") that particles remained stable during incubation at the given temperature. I.A denotes immediate aggregation.
[b] PBS: phosphate buffer saline; OBM: Oxidative burst medium; OBM: Oxidative burst medium

The degree of acetylation and the molecular weihght of chitosan have a direct influence on the size, zeta potential and stability of chitosan-based nanoparticles. This was evidenced in ionically crosslinked nanoparticles and in nanogels produced by reverse emulsion. The ionically crosslinlked particles are far more stable when the degree of acetylation of chitosan increases (up to 56 %).

Francisco M Goycoolea*, Fabrice Brunel, Nour E El Gueddari, Anna Coggiola, Giovanna Lollo, Bruno M Moerschbacher, Carmen Remuñán-López, Thierry Delair, Alain Domard and María J Alonso*

Physical properties and stability of soft gelled chitosan-based nanoparticles

ToC